Assessment of the potential of cold plasma-pretreated beta-tricalcium phosphate in combination with periodontal ligament stem cells to enhance bone regeneration in vivo

M Miletić (maja.miletic@stomf.bg.ac.rs)
University of Belgrade, School of Dental Medicine
N Puač
University of Belgrade, Institute of Physics
N Škoro
University of Belgrade, Institute of Physics
B Brković
University of Belgrade, School of Dental Medicine
M Andrić
University of Belgrade, School of Dental Medicine
BB Prokić
University of Belgrade, Faculty of Veterinary Medicine
V Danilović
University of Belgrade, School of Dental Medicine
S Milutinović-Smiljanić
University of Belgrade, School of Dental Medicine
O Mitrović-Ajtić
University of Belgrade, Institute for Medical Research
S Mojsilović
University of Belgrade, Institute for Medical Research

Research Article

Keywords: β-TCP, cold atmospheric plasma, mesenchymal stromal/stem cells, bone regeneration

Posted Date: November 4th, 2022

DOI: https://doi.org/10.21203/rs.3.rs-2206274/v1

Abstract

Objectives

A new strategy in the field of regenerative bone tissue medicine involves the combination of artificial bone substitutes and progenitor cells. In this approach the positive interaction of biomaterials and cells is crucial for successful bone regeneration.

Materials and methods

Herein, we examined if cold atmospheric plasma (CAP)-pretreated beta-tricalcium phosphate (β-TCP) alone, or in combination with periodontal ligament stem cells (PDLSCs), increases the bone regeneration in rabbit calvarial critical-size defect model. After two and four weeks of bone regeneration we analyzed and compared the bone formation in experimental groups using histology and histomorphometry. In addition, we used immunohistochemistry to analyze the protein expression of bone healing markers.

Results

After two and four weeks of bone regeneration, the results of histological and histomorphometric, analysis demonstrated significantly higher bone regeneration capacity and absence of inflammatory reaction in the implant of plasma-treated β-TCP in combination with PDLSCs compared to the β-TCP alone. Furthermore, immunohistochemical analysis showed the highest percentages of immunostained cells for the bone healing markers, bone morphogenic proteins 2 and 4, runt-related transcription factor 2, collagen-1, and osteonectin in the defects filled with CAP-treated β-TCP and PDLSC which additionally support beneficial therapeutic effects of such combined approach on osteoregeneration.

Conclusion

The CAP-pretreated β-TCP implant seeded with PDLSCs shows significantly higher bone regeneration capacity and absence of inflammatory reaction in vivo in comparison to the β-TCP alone.

Clinical relevance

Cold atmospheric plasma could be an effective method of treating β-TCP to improve the interaction of the material with stem cells enhancing regeneration of the bone.

Introduction

Bone regeneration is a complex process involved in normal remodeling and healing of bone following surgery or trauma. However, significant damage, exceeding the normal reparatory potential of the bone, results in the formation of residual defects, which is particularly common in oral and maxillofacial regions. Such defects lead to the functional and esthetic impairment, significantly affecting quality of life of affected individuals.

Autologous bone is still considered as a standard for bone regeneration, since it exerts osteoconductive, osteoinductive and osteogenic features. Still, its usage is limited by the amount of available bone and the need for a second surgical site to obtain the graft [1], which is the reason why numerous bone substitute materials were developed, aiming to overcome these limitations.

Alloplastic bone substitutes are synthetic materials composed of chemical components of native bone. Typical examples are different types of hydroxyapatite and calcium phosphate, including beta tricalcium phosphate (β-TCP). These materials have osteoconductive features, meaning that they act as a scaffold for influx of osteogenic cells, but themselves do not have any osteoinductive or osteogenic ability. On the other hand, application of alloplastic materials is not hindered by limitations in quantity, and neither carries the risk of infectious disease transmission [2].

A new strategy in the field of regenerative bone tissue medicine involves the combination of artificial bone substitutes, carriers and progenitor cells such as mesenchymal stem/stromal cells (MSCs) or mature bone cells [3–5]. MSCs are multipotent cells that are found in almost all tissues and have the ability to self-renew and differentiate in the direction of different specialized cell types. Multipotent differentiation ability, secretion of paracrine tropic factors and immunomodulatory properties make these cells ideal candidates for use in regenerative medicine and tissue engineering [6]. Dental tissue is an easily accessible and rich source of these cells, and the findings of various studies indicate the possibility of their use in the repair and/or regeneration of bone, cartilage, hard dental tissues, etc. [7, 8]. Dental tissue derived MSCs include dental pulp stem cells (DPSCs), stem cells from human exfoliated deciduous teeth (SHEDs), dental follicle stem cells (DFSCs), and periodontal ligament stem cells (PDLSCs) [9]. MSCs transplants together with calcium phosphate-based biomaterials have been shown to significantly increase osteogenesis, promote angiogenesis, and accelerate material degradation [10–12].

Recent research has shown that biomaterials, depending on their physicochemical properties, can modify the microenvironment of cells and trigger regulatory signals that induce the differentiation of these cells into specific cell lines. Surface characteristics of materials, such as chemical composition, hydrophilicity, surface energy and topography are key factors that control the behavior of cells on the surface of biomaterials [13, 14].Various studies in recent years have shown that all these properties can be very easily modified by treatment with cold atmospheric plasma (CAP) [15–18].

Along with well-established processing by cold plasmas established at low pressures [19], cold plasmas at atmospheric pressure have paved the way towards efficient processing of different materials. In principle, this plasma provides an active chemical environment at near room temperature and at atmospheric pressure enabling physical and chemical interaction with the surface of materials – such as

etching, deposition, activation etc. [20]. It is now well known that cold plasmas at atmospheric pressure generate a diversity of reactive oxygen (ROS) and nitrogen species (RNS) such as radicals, ions, excited atoms and molecules (O, OH, H_2O_2, O_3, N_2*, O_2^- etc.) [21]. Thus, atmospheric pressure plasmas established as a prosperous technology in the medical field with varied applications ranging from sterilization of medical equipment, and surface modification of biomaterials, to the treatment of wounds and tissues [22–24]. Many plasma sources can operate in ambient air, without the addition of any noble gasses, highlighting the biggest advantage of this technology – the generation of a highly reactive plasma chemical environment that can be brought into immediate contact with the substrate treatment. Most of these plasma sources belong to the dielectric barrier discharge (DBD) type [25, 26]. The main asset of a DBD source is the possibility to provide a large effective surface for treatment in comparison to the other plasma sources operating at atmospheric pressure. Investigation of properties of DBD sources has been performed providing ample information for employment in different types of applications [27–30]. However, applications related to plasma treatments of (bio)material surfaces, i.e., bone grafting material, are infrequent and in most cases performed using low-pressure plasma systems [15, 31–33]. Having in mind a potential of CAP to induce changes to the treated biomaterials [34, 35], it can be utilized as an excellent tool for enhancing properties of graft materials.

In this study we aimed to examine if pretreatment of β-TCP with CAP, alone or in combination with PDLSCs, increases the regeneration of critical size bone defects in calvaria of rabbits.

Material And Methods

Experimental material and cells

Periodontal ligament stem cells were isolated using the explant method, as previously described [36] from periodontal tissues of the healthy third molars extracted from patients undergoing orthodontic treatment at the Department of Oral Surgery of the School of Dental Medicine. The procedures were following the approved set of ethical guidelines by the Ethics Committee of the Faculty of Dental Medicine, University of Belgrade, after obtaining informed consent from patients. After isolation, PDLSCs were cultured in DMEM (Sigma-Aldrich, St. Luis, MO, USA) supplemented with 10% fetal bovine serum (FBS; Capricorn Scientific, Germany), and 100 U/ml penicillin and 100 μg/ml streptomycin (PAA Laboratories) and passaged regularly. For these experiments, passage P4 was used. The characterization of PDLSCs was done by phenotype analysis using flow cytometry (CyFlow SL, Partec, Munster, Germany) and by culturing cells in specific differentiation medium (osteogenic, chondrogenic, adipogenic) to show their multidifferentiation potential, as reported previously [36].

As the scaffold material, synthetic β-tricalcium phosphate granules (β-TCP), size 0.5-1mm (R.T.R. Syringe, Septodont, France) were used. For seeding onto the scaffold, the cells from passage 4 were detached by using 0.05% trypsin with 1 mM EDTA (PAA Laboratories), counted in trypan blue (PAA Laboratories), and 2×10^5 cells were seeded onto CAP-treated or untreated βTCP granules immediately before the implantation.

Plasma Source

In this work, we used a surface dielectric barrier discharge (SDBD) system that operates in air at atmospheric pressure for the treatment of β-TCP. The plasma source consisted of a glass upper part with powered and grounded segmented electrodes. It was placed above a grounded metallic surface covered with a glass dielectric plate (90 mm in diameter) that serves as a sample holder (Fig. 1a). The distance between the upper and lower electrode surfaces was d = 2.5 mm. In the upper part electrodes, made of 5 mm wide copper tape were placed on both sides of a 2 mm thick glass dielectric plate in an alternating manner (see Fig. 1a). The copper stripes fixed to the bottom of the upper glass plate (facing the sample holder) were powered while the stripes at the top were grounded. Powered electrodes were connected to 50 Hz sine high-voltage signal that was monitored by using high-voltage probe while the discharge current was obtained by measuring voltage drop on a 15 kΩ resistor. In Fig. 1b we show waveforms of the voltage and current obtained during the treatment. The spikes visible in the current signal minimum and maximum values belong to numerous microfilaments that are formed between the powered electrode and the dielectric on the sample holder. However, observed with the naked eye the discharge appeared diffuse due to the large number and density of the filaments so we can assume that the treatment of samples was uniform.

Animal Experiment Surgery Procedure And Study Design

Experimental procedures were approved by the Ethical Committee of the Faculty of Veterinary Medicine, University of Belgrade and Ministry of Agriculture, Forestry and Water Management of the Republic of Serbia (No. 323-07-08477/2015-05/3). Ten 4-month-old Chinchilla rabbits weighing between 3.5 and 4.3 kg were used in this study. Before the experimental procedure animals underwent examination and a 14-days-accommodation protocol. Rabbits were housed in individual cages. In all phases of the experiment the animals had free access to food and water and were under the following conditions: temperature 21 ± 1,5°C, air humidity 53 ± 4%, 15 air changes/h, with artificial lighting at intervals of 12 h day/night.

Enrofloxacin (Baytril 2.5%, Bayer, Germany) 10 mg/kg i.m. was used in premedication and in 5 postoperative days, as well as butorphanol (Butomidor 10 mg/ml, Richter Pharma Ag, Austria) 0.5 mg/kg s.c. for pain management.

In all animals, general anesthesia was induced using intramuscular injection of 35 mg/kg of ketamine hydrochloride (Ketamidor 10%, Richter Pharma AG, Austria) and 5 mg/kg of xylazine (Xylased 20 mg/ml, Bioveta, Czech Republic). After intubation, anesthesia was maintained with sevoflurane (Sevorane, 100%, Abbvie biopharmaceuticals GMBH). Anesthetized rabbits were placed in a face down position on the operating table. The surgical site was shaved and then cleaned with 70% isopropyl alcohol. Final skin preparation was done with povidone iodine (Betadine, Alkaloid AD Skopje). The midline incision of the scalp, created between the base of the ears and approximately 5 cm anteriorly, was done for the full-thickness skin flap. Parietal bones were exposed after sharp subperiosteal dissection of the pericranium. Four full-thickness calvarial critical-sized defects, measuring 8 mm in diameter, were created with

electrical drilling under copious saline irrigation, two of them on each side of the midline of the parietal bone (Fig. 2a). Surgical template, made of the sterile acrylic disk, was used to ensure each defect was identical.

In every rabbit, each of the 4 defects was randomly allocated to one of the following study groups that are summarized in Table 1.

Table 1
Description of study groups.

Group	β-TCP	Stem Cells
I	untreated	-
II	plasma treated	-
III	untreated	PDLSC
IV	plasma treated	PDLSC

The bone substitutes filled the bone defects from the dura to the level of marginal bone replacing the volume of the removed bone and the pericranium (Fig. 2b) and skin were sutured in layers with absorbable sutures. The surgical wound was treated once with Engemycin Spray (Intervet Productions S.r.l., Italy). During the postoperative animal care rabbits were observed twice a day until the end of the experiment. Sutures were removed 12 days after the surgery. For pain assessment the Rabbit Grimace Scale of the National center for the replacement, refinement & reduction of animals in the research scale of the Newcastle University was used.

One rabbit died postoperatively, while the remaining animals (five after 2 weeks and four at 4 weeks postoperative) were anesthetized by the protocol and then euthanized with intravenous application of 150 mg/kg sodium pentobarbitone. Calvarial bones were surgically removed and separated into different bone blocks according to study groups.

Histological And Histomorphometric Analysis

The 36 bone specimens were kept in 4% formaldehyde in 0.1 M phosphate-buffered saline solution (pH 7.2) for 48h. Specimens were decalcified using formic acid, washed in running water, and gradually dehydrated in a series of ethanol solutions. Then each specimen was embedded in paraplast, sectioned in 4 μm thick slices by rotary microtome (Leica Sand M2000R, Leica Microsystems, Wetzlar, Germany). Thereafter, the preparations were de-waxed, processed to Hematoxylin-Eosin (HE) and analyzed under a light microscope. Special staining with Trichrome Goldner was used to allow us to distinguish between mineralized bone that was displayed in the green spectrum and non-mineralized bone that was displayed in the red spectrum.

The histological parameters were evaluated at 40 x magnification under a microscope (Leitz Labor Lux S Fluorescence Microscope, Ernst Leitz Wetzlar GMBH, Germany), with exception of inflammatory cell infiltrates which were counted on total magnification of 400x. 2D images were captured at 40-400x magnification using a digital color camera (Leica DFC295, Germany) and merged to create a single image for each histological section. Thereafter, images were analyzed using software (Leica University Suite, version 4.3, Leica Microsystems, Germany) running on a personal computer.

The histomorphometric parameters we evaluated were the presence and area of: 1) newly formed bone tissue; 2) mineralized and non-mineralized bones (osteoids); 3) newly formed connective tissue; 4) non resorbed bone graft particles; 5) blood vessels. All histomorphometric results were presented as a percentage.

The presence of an inflammatory reaction was determined based on the number of inflammatory infiltrate cells (macrophages, giant cells, lymphocytes, plasma cells and neutrophilic granulocytes) and classified as mild (0–5 cells), moderate (6–10 cells), or severe (11 or more)). For each sample, three histological fields of the same surface (10,000 μm^2) per section, with a spacing of 50 μm between fields, at 400x magnification, were analyzed.

Immunohistochemical Analysis

For the immunohistochemical analysis, the paraffin tissue sections were analyzed cut at 5 μm, and the slides were heated for 60 min at 56°C. Prior to the antigen retrieval step, the sections were deparaffinized and rehydrated through a series of xylenes and alcohols. To block endogenous peroxidase activity, tissue sections were treated with 3% H_2O_2 solution in PBS. For epitope retrieval, tissue sections were heated in a microwave oven for 21 min., at 680 W, in 10 mmol/L citrate buffer, pH 6.0.

The tissue sections were incubated overnight, at + 4°C, in the humid chamber with appropriate antibodies (dilution 1:200) against osteonectin (anti-SPARC antibody, Code: ABIN190339, Antibodies Online), Runt-Related-Transcription Factor 2 (RUNX, Code: ABIN2780589), collagen type 1 (Code: ABIN 153357), bone morphogenic protein (BMP)-2 (Code: ABIN730903) and BMP-4 (Code: ABIN 223638). Streptavidin-biotin technique was used for immunostaining ($LSAB^+$/HRP Kit, Peroxidase Labeling, K0690, DAKO Cytomation, Glostrup, Denmark). Immunoreactivity complex was visualized with DAKO Liquid DAB^+ Substrate/Chromogen System (Dako, CA, USA, Code No. K3468) and then counterstained with Mayer's hematoxylin (Merck, KGaA, Darmstadt, Germany). The tissue sections with omitted primary antibodies served as a negative control. For positive control, the tissue sections that were known to express osteonectin, RUNX, BMP-2, BMP-4 and collagen 1 were used. BMP-2, BMP-4, collagen 1, RUNX2 and osteonectin positive cells in tissues were analyzed by a light microscope (Olympus AX70, Hamburg, Germany) with 40× magnification. In all analyzed samples of tissue, five hot spots were selected for image analysis in ImageJ (The National Institutes of Health, Bethesda, MD, USA). BMP-2, BMP-4, collagen 1, RUNX2 and osteonectin expressions were calculated by determining the positive areas (brown-colored

cells) per microscopic field (40× magnification), based on the threshold. Median values of BMP-2, BMP-4, collagen 1, RUNX2 and osteonectin immunostaining were calculated for each individual tissue sample.

Statistics

Statistical analysis was performed using SPSS for windows - version 18.0 software (SPSS, Inc., Chicago, IL, USA). All data were presented as the mean ± SD. Two-way ANOVA was performed at 95% level of significance, followed by LSD post hoc comparisons.

Results

Histological and histomorphometric analysis

In all examined samples, two weeks after the surgical intervention, we determined that the healing went smoothly, without signs of necrosis, infection and bleeding. We also found that in all samples the central part of the surgical defect was filled with newly formed connective tissue, in which the bone graft particles were located. In all samples, we observed early ossification centers, which were located on the graft surface. As expected, the number of ossification foci was higher in the peripheral areas of the defect, near the "old" bone, and lower in the central areas of the defect. The newly formed bone had the properties of immature, fibrous bone, which is the expected result for this evaluation period. The results of histomorphometric analysis after 2 weeks of healing are shown in Table 2.

Table 2
Results on histomorphometric analysis after 2 weeks for different study groups

Group	Total bone %	Mineralized bone %	Non-mineralized bone%	Connective tissue%	Graft particles %	Blood vessels %
I	5.55 ± 1.30	5.16 ± 1.01	0.39 ± 0.29	61.89 ± 15.00	41.85 ± 6.46	0.57 ± 0.35
II	8.77 ± 2.80	6.77 ± 1.94	2.00 ± 0.85	**42.86 ± 6.83 ***	47.39 ± 5.74	0.97 ± 0.42
III	**17.52 ± 7.78 ** ##**	**16.93 ± 4.23 * #**	**0.60 ± 0.34 #**	**41.40 ± 4.56 ***	39.84 ± 8.72	1.25 ± 0.55
IV	**23.53 ± 7.63 ** ##**	**21.03 ± 4.73 ** ##**	**2.50 ± 0.33 ***	**48.53 ± 2.53 #**	**26.99 ± 1.8 ##**	0.95 ± 0.27

* $p < 0.05$; ** $p < 0.01$ in comparison with control (group I); # $p < 0.05$; ## $p < 0.01$ in comparison with group II.

Histomorphometric analysis showed that the highest degree of bone regeneration was achieved in the groups III and IV. The percentage of total bone surface area, particularly its mineralized fraction, as the most important parameter of bone regeneration, was statistically significantly higher in these two groups in relation to the groups I and II.

We did not observe a severe inflammatory reaction in any of the examined groups. In groups I and II the inflammatory reaction was moderate. In all the tested samples of group IV and in 75% of group III we noticed either complete absence of inflammatory infiltrate cells or it was minimal.

Four weeks after surgery in all examined groups, the central part of the defect was still filled with newly formed connective tissue in which there were unintegrated graft particles, while in areas that are more peripheral signs of graft integration were observed. The results of histomorphometry showed that the total amount of newly formed bone (mineralized and non-mineralized fraction) was statistically significantly higher in groups III and IV, when compared to group I. In groups III and IV, there was a reduction in the area occupied by graft particles. The results of the histomorphometric analysis are listed in Table 3.

Table 3
Results on histomorphometric analysis after 4 weeks for different study groups.

Group	Total bone %	Mineralized bone %	Non-mineralized bone%	Connective tissue%	Graft particles %	Blood vessels %
I	4.87 ± 1.40	4.17 ± 1.38	0.70 ± 0.23	48.77 ± 2.06	47.75 ± 0.71	0.61 ± 0.38
II	11.89 ± 2.77	7.39 ± 1.81	2.44 ± 0.81	52.98 ± 3.72	36.61 ± 4.81	0.58 ± 0.26
III	**24.34 ± 7.46 ** **	**15.33 ± 6.23 * **	**9.02 ± 3.43 ** **	47.19 ± 4.72	**29.75 ± 10.53 * **	0.57 ± 0.38
IV	**21.32 ± 4.82** **	**14.71 ± 2.79 * **	**6.61 ± 2.16 * **	53.51 ± 4.67	**14.35 ± 1.80 * **	0.99 ± 0.35

* $p < 0.05$; ** $p < 0.01$ in comparison with control (group I)

Additionally, there was a decrease in the number of inflammatory infiltrate cells compared to the two-week evaluation period, so 75% of the samples of groups I and II had moderate inflammatory infiltrate, and 25% of the samples in these groups, as well as 100% of the samples of groups III and IV showed complete absence or signs of minimal inflammatory reaction.

Immunohistochemical Analysis

According to our results, two weeks after surgery, the highest number of BMP-2 positive cells was identified in group IV (Fig. 3d). Immunohistochemical analysis showed a significant increase in positively stained BMP-2 cells in group IV in comparison to groups I, II, and III ($p < 0.001$) (Fig. 3).

After 4 weeks of surgery, we observed a significantly higher number of BMP-2 positive cells between groups III and IV in comparison to group I ($p < 0.001$), as well as in group IV in comparison to group II ($p < 0.001$) (Fig. 3).

Two weeks postoperatively, the number of BMP-4 immunopositive cells detected in group IV (Fig. 4d) was higher than in groups I, II ($p < 0.001$), and III ($p < 0.05$). A significantly higher number of BMP-4 positive cells was also detected in group III when compared to group I ($p < 0.05$) (Fig. 4).

After four weeks, a significantly higher number of BMP-4 positive cells was noticed in group IV in comparison to groups I ($p < 0.01$) and II ($p < 0.001$) (Fig. 4).

Runx-2 immunopositive cells dominated in group IV, both after two and four weeks after surgery (Fig. 5d and 5h). We detected a significantly higher number of Runx-2 immunopositive cells in group IV in comparison to group I after two weeks and after four weeks in comparison to groups I and II ($p < 0.05$) (Fig. 5).

The number of Collagen 1 cells, after two weeks, was significantly higher in groups II, III, and IV when compared to group I ($p < 0.001$).

Collagen 1 immunohistochemical staining showed that the highest number of positive cells was four weeks after surgery in group IV (Fig. 6h) and significantly more compared to group III ($p < 0.01$) (Fig. 6).

Two weeks postoperatively, we did not find any significant difference in the number of osteonectin positive cells between the four groups. However, after four weeks, the number of positive cells in groups II ($p < 0.001$) and IV ($p < 0.01$) were significantly higher compared to group I. Also, combination of β-TCP, plasma and PDLSCs (group IV) significantly increased the number of osteonectin immunopositive cells in comparison to β-TCP and PDLSCs (group III) ($p < 0.05$) (Fig. 7).

Discussion

The objective of this study was to investigate if pretreatment of β-TCP with cold plasma alone or in combination with PDLSCs enhances bone regeneration. To that end, a well-established rabbit calvarial critical-size defect model was used [37]. After two and four weeks of bone regeneration we analyzed and compared the bone formation in experimental groups using histology and histomorphometry. In addition, we used immunohistochemistry to analyze the protein expression of bone healing markers. The results of the present study showed significantly higher bone regeneration capacity and absence of inflammatory reaction in the implant of plasma-treated β-TCP in combination with PDLSCs compared to the β-TCP alone.

Despite the great regenerative capacity of bone tissue, critical size defects cannot be repaired without therapeutic intervention. In the last decades, many novel therapeutic strategies have been developed to improve bone regeneration [38]. Recent bone tissue engineering approaches based on seeding osteogenic cells onto calcium phosphate ceramic scaffolds have tried to enhance new bone tissue formation [39]. Among all the different types of progenitor cells, MSCs are the most commonly used population in various fields of regenerative medicine, including bone regeneration [40, 41]. Dental-derived MSCs possess the similar multipotent potential and immunoregulatory capacities as bone marrow-derived MSCs, which have been usually applied to seed biomaterials in numerous pre-clinical and clinical studies [42–45]. The advantages of hPDLSC over other MSCs from dental tissue are reflected in easier availability, lower donor site morbidity, and lower requirements for invasive surgery [46]. It was reported that PDLSCs have osteogenic potential and show better regeneration capability and multipotency compared to other subpopulation of dental-derived stem cells, and thus represent an optimal alternative to BM-MSCs as a source of cells used in bone repair [46–49].

The regenerative properties of β-TCP besides other bioceramic materials are distinct and commonly used in bone regeneration [50]. β-TCP possesses good biocompatibility, osteoconductivity, fast resorption rate, and a high rate of solubility [51]. Physical characteristics of β-TCP, like surface roughness, porosity, and pore sizes, can be adjusted to optimize new bone formation. Moreover, the addition of cells and/or cell-derived active substances can further promote the osteoinductive capacity of the graft [4].

According to the results of our study, histological and histomorphometric analysis demonstrated that seeding of PDLSCs onto β-TCP, both untreated and pretreated with CAP, led to improved osteo-regeneration capacity in comparison to β-TCP without the cells. Namely, the percentage of the total bone area, as well as the mineralized bone, was significantly increased in groups III and IV, compared to groups without the cells (groups I and II), already two weeks after treatment, and after four weeks we showed a significant reduction in the amount of the residual graft particles as well, indicating better resorption of β-TCP and intensive integration into bone tissue. This resorption was greater in group IV compared to group III, although without statistical significance. Additionally, we observed better vascularization in group IV after four weeks, but this period was not enough to show statistical significance. As for the inflammatory reaction, our results showed that after two weeks most of the sites that were treated with PDLSCs had minor or no inflammatory reaction, compared to the groups without the cells in which the inflammation was moderate up to the fourth week.

In addition to histological examination of tissue samples, in order to more finely determine bone formation, we assessed expression of several osteogenic markers, namely BMP-2, BMP-4, collagen-1, Runx-2, and osteonectin, by immunohistochemical staining. Bone morphogenic proteins belong to the TGF-β superfamily and are involved in both initiation and in terminal osteogenic differentiation [52–56]. Among other family members, BMP-2, 4, 6, 7, and 9 are especially important for bone formation, as they induce a signaling cascade involving Runx-2 transcription factor to increase osteoprogenitor cell proliferation, differentiation and synthesis of ECM production [57]. Collagen-1 is the main component of the bone ECM and is also expressed at the earliest stages of osteogenesis [58, 59], while osteonectin is a

glycoprotein expressed in more mature osteoblasts that binds Ca, initiate mineralization and cell-ECM interaction [60].

We observed the highest percentages of immunostained cells for the tested markers in the defects filled with CAP-treated β-TCP and PDLSCs which additionally support beneficial therapeutic effects of such combined approach on osteoregeneration. BMP-2, -4, collagen-1, and Runx-2 increased already two weeks after the implantation of the plasma-treated material seeded with the cells. Plasma treatment itself has shown some level of improved osteogenesis, as collagen-1 and osteonectin expression have increased after four weeks in the CAP-treated groups (II and IV) in comparison to the corresponding groups with untreated material, with or without hPDLSC (I and III).

The positive interaction of biomaterials and cells are crucial for successful bone regeneration. Research have shown that the surface characteristics of calcium phosphates, like chemical composition, molecular weight, surface properties, including hydrophilicity and topography, can positively affect stem cell functions such as the adhesion, proliferation and differentiation [4, 61]. Even though a few studies have investigated the influence of plasma-treated biomaterial surfaces on pro-osteogenic cell activities *in vitro* [17, 62, 63], to best our knowledge, there are no research that explored *in vivo* effects of surface-modified CaP biomaterials in combination with MSCs on bone regeneration.

Canullo *et al*. (2018) have demonstrated that argon plasma surface modification of HA and calcium phosphate ceramics increases the protein adsorption and murine osteoblasts adhesion [63]. Choi *et al*. (2013) also showed an increased attachment and proliferation of MC3T3 mouse osteoblasts after treatment of HA/β-TCP with nitrogen and air CAP [17]. This can be achieved by increasing the hydrophilicity of the scaffold surface. It has been reported that when a surface is treated with CAP, carbon levels decrease and oxygen functional groups levels increase, which results in a more polar and hydrophilic surface [15–17, 64]. The hydrophilicity of a surface is, on the other hand, essential for the adsorption of extracellular matrix (ECM) proteins and hence the adhesion of cells via cell-ECM interactions [65]. In addition, it has been reported that hydrophilic surfaces increase the adhesion and proliferation of osteoblasts, and promote maturation and differentiation of bone precursor cells, creating a pro-osteogenic microenvironment [66]. Osteogenic precursors cultured on these surfaces produce more differentiation markers, such as ALP and osteocalcin, and increased levels of local factors, like PGE2 and TGF-β [67]. On the other hand, the hydrophilicity and microporosity of surfaces also affects macrophage activity [10, 68]. The increased surface energy of hydrophilic surfaces enhances the release of anti-inflammatory markers by macrophages and modulates their polarization to anti-inflammatory phenotype [69, 70]. It has been also shown that surface topography influences gene expression and cytokine secretion profile of MSCs and enhances their osteogenic differentiation capacity [71, 72].

The implanted MSCs do not survive long at the implantation site, but initiate the bone regeneration process by recruiting host MSCs and osteoprogenitors, helping to resolve inflammation, and favoring M2 macrophage and osteoclast differentiation that both promote osteogenesis [73, 74]. As a way of modulating the immune response, MSCs induce macrophage polarization towards an anti-inflammatory

and reparatory M2 phenotype [75]. They also suppress Th1 and cytotoxic T cell proliferation and function, favoring Th2 and Treg cell polarization, inhibit NK cell cytotoxicity and induce tolerogenic DC generation. This immunosuppressive effect is crucial for terminating the inflammatory phase and moving to the regenerative phase, avoiding chronic inflammation, which is detrimental to any tissue regeneration [10]. M2 macrophages, on the other hand, support MSC proliferation and differentiation into osteoblasts [76]. Moreover, M2 macrophages, and osteoclasts by phagocytosis and creating an acidic environment, lead to resorption of CaP materials and release of Ca and phosphate ions [51], which contribute to MSC osteogenic differentiation and mineralization [77]. Previous studies have shown that macrophage recruitment to an implanted CaP is significantly enhanced when the CaP scaffold is seeded with MSCs [10, 74, 78].

Based on these studies and our results we can speculate that surface modification of β-TCP by CAP leads to improved adhesion and interaction of MSCs with the material and surrounding host tissue and cells, leading to the transition of pro-inflammatory to the pro-reparatory microenvironment. Even though this study has its limitations, such as lack of physico-chemical analysis of CAP-treated material, a limited number of experimental animals and follow-up time, and lack of some relevant histochemical markers of vascularization and inflammation, our findings suggest that treatment with cold atmospheric plasma is a very easy and effective method of treating β-TCP, which improves the interaction of the material with stem cells and thus improves bone regeneration.

Declarations

Ethical Approval

All protocols for animal experiments were approved by the Faculty of Veterinary Medicine, University of Belgrade and Ministry of Agriculture, Forestry and Water Management of the Republic of Serbia (No. 323-07-08477/2015-05/3). Periodontal ligament stem cells were obtained from healthy volunteers after the approval by the Ethics Committee of the School of Dental Medicine, University of Belgrade (No. 36/13) and upon providing informed consent of donors.

Competing interests

The authors declare no competing interests.

Authors' contributions

M.M. and S.M. conceived the ideas and are responsible for the conception and design of the study. Acquisition of data and interpretation as well as writing of the manuscript were conducted as leading researchers. N.P. and N.S. were responsible for every aspect of CAP settings and the treatments of the material, as well as in the writing of the manuscript. B.B. and M.A. performed the surgical intervention and gave intellectual content. B.B.P. was responsible for animal care and editing of the manuscript. V.D. and S.M.S. were responsible for histologic and histomorphometric analysis and statistical analysis of the

results. They also participated in the writing and reviewing of the manuscript. O.M.A. performed imunochistochemical and statistical analysis, prepared figures, and gave input to the manuscript.

Funding

The study was supported by the Ministry of Education, Science and Technological Development of the Republic of Serbia, contract No. 451-03-68/2022-14/200129 (M.M., B.B., M.A., S.M.S., V.D.), 451-03-68/2022-14/200015 (S.M., O.M.A.), 451-03-68/2022-14/200024 (N.P., N.S.), 451-03-9/2021-14/200143 (B.B.P.).

Availability of data and materials

The data presented in this study are available from the corresponding author upon reasonable request.

References

1. Laurencin C, Khan Y, El-Amin SF (2006) Bone graft substitutes. Expert Review of Medical Devices 3(1):49–57. https://doi.org/10.1586/17434440.3.1.49
2. Fukuba S, Okada M, Nohara K, Iwata T, Iwata T (2021) Alloplastic Bone Substitutes for Periodontal and Bone Regeneration in Dentistry: Current Status and Prospects. Materials 14(5):1096. https://doi.org/10.3390/ma14051096
3. Aghali A (2021) Craniofacial Bone Tissue Engineering: Current Approaches and Potential Therapy. Cells 10(11):2993. https://doi.org/10.3390/cells10112993
4. Gao C, Peng S, Feng P, Shuai C (2017) Bone biomaterials and interactions with stem cells. Bone Res 5(1):17059. https://doi.org/10.1038/boneres.2017.59
5. Laurencin CT, Khan Y (2012) Regenerative Engineering. Sci Transl Med 4(160). https://doi.org/10.1126/scitranslmed.3004467
6. Kangari P, Talaei-Khozani T, Razeghian-Jahromi I, Razmkhah M (2020) Mesenchymal stem cells: amazing remedies for bone and cartilage defects. Stem Cell Res Ther 11(1):492. https://doi.org/10.1186/s13287-020-02001-1
7. Ercal P, Pekozer GG, Kose GT (2018) Dental Stem Cells in Bone Tissue Engineering: Current Overview and Challenges. In: Turksen K (ed) Cell Biology and Translational Medicine, Volume 3. Springer International Publishing, Cham, pp 113–127
8. Soudi A, Yazdanian M, Ranjbar R, Tebyanian H, Yazdanian A, Tahmasebi E, Keshvad A, Seifalian A (2021) Role and application of stem cells in dental regeneration: A comprehensive overview. EXCLI Journal; 20:Doc454; ISSN 1611-2156. https://doi.org/10.17179/EXCLI2021-3335
9. Okić-Đorđević I, Obradović H, Kukolj T, Petrović A, Mojsilović S, Bugarski D, Jauković A (2021) Dental mesenchymal stromal/stem cells in different microenvironments— implications in regenerative therapy. WJSC 13(12):1863–1880. https://doi.org/10.4252/wjsc.v13.i12.1863

10. Humbert P, Brennan MÁ, Davison N, Rosset P, Trichet V, Blanchard F, Layrolle P (2019) Immune Modulation by Transplanted Calcium Phosphate Biomaterials and Human Mesenchymal Stromal Cells in Bone Regeneration. Front Immunol 10:663. https://doi.org/10.3389/fimmu.2019.00663
11. Shi H, Zong W, Xu X, Chen J (2018) Improved biphasic calcium phosphate combined with periodontal ligament stem cells may serve as a promising method for periodontal regeneration. Am J Transl Res 10(12):4030–4041
12. da Silva AAF, Rinco UGR, Jacob RGM, Sakai VT, Mariano RC (2022) The effectiveness of hydroxyapatite-beta tricalcium phosphate incorporated into stem cells from human exfoliated deciduous teeth for reconstruction of rat calvarial bone defects. Clin Oral Investig 26(1):595-608. https://doi.org/10.1007/s00784-021-04038-9
13. Cui H, Wang X, Wesslowski J, Tronser T, Rosenbauer J, Schug A, Davidson G, Popova AA, Levkin PA (2021) Assembly of Multi-Spheroid Cellular Architectures by Programmable Droplet Merging. Adv Mater 33(4):2006434. https://doi.org/10.1002/adma.202006434
14. Tirrell M, Kokkoli E, Biesalski M (2002) The role of surface science in bioengineered materials. Surface Science 500(1–3):61–83. https://doi.org/10.1016/S0039-6028(01)01548-5
15. Choy CS, Lee WF, Lin PY, Wu Y-F, Huang H-M, Teng N-C, Pan Y-H, Salamanca E, Chang W-J (2021) Surface Modified β-Tricalcium phosphate enhanced stem cell osteogenic differentiation in vitro and bone regeneration in vivo. Sci Rep 11(1):9234. https://doi.org/10.1038/s41598-021-88402-5
16. Moriguchi Y, Lee D-S, Chijimatsu R, Thamina K, Masuda K, Itsuki D, Yoshikawa H, Hamaguchi S, Myoui A (2018) Impact of non-thermal plasma surface modification on porous calcium hydroxyapatite ceramics for bone regeneration. PLoS ONE 13(3):e0194303. https://doi.org/10.1371/journal.pone.0194303
17. Choi Y-R, Kwon J-S, Song D-H, Choi EH, Lee Y-K, Kim K-N, Kim K-M (2013) Surface modification of biphasic calcium phosphate scaffolds by non-thermal atmospheric pressure nitrogen and air plasma treatment for improving osteoblast attachment and proliferation. Thin Solid Films 547:235–240. https://doi.org/10.1016/j.tsf.2013.02.038
18. Wagner G, Eggers B, Duddeck D, Kramer FJ, Bourauel C, Jepsen S, Deschner J, Nokhbehsaim M (2022) Influence of cold atmospheric plasma on dental implant materials - an in vitro analysis. Clin Oral Investig 26(3):2949-2963. https://doi.org/10.1007/s00784-021-04277-w
19. Makabe T, Petrovic ZLj (2014) Plasma Electronics, 2 edn. CRC Press, Boca Raton. https://doi.org/10.1201/b17322
20. Keidar M, Weltmann K-D, Macheret S (2021) Fundamentals and Applications of Atmospheric Pressure Plasmas. Journal of Applied Physics 130(8):080401. https://doi.org/10.1063/5.0065750
21. Fridman A (2008) Plasma Chemistry, 1st edn. Cambridge University Press
22. Moisan M, Barbeau J, Crevier M-C, Pelletier J, Philip N, Saoudi B (2002) Plasma sterilization. Methods and mechanisms. Pure and Applied Chemistry 74(3):349–358. https://doi.org/10.1351/pac200274030349

23. Lu X, Reuter S, Laroussi M, Liu D (2019) Nonequilibrium Atmospheric Pressure Plasma Jets: Fundamentals, Diagnostics, and Medical Applications, 1st edn. CRC Press, Boca Raton : CRC Press, Taylor & Francis Group, [2019]
24. von Woedtke Th, Reuter S, Masur K, Weltmann K-D (2013) Plasmas for medicine. Physics Reports 530(4):291–320. https://doi.org/10.1016/j.physrep.2013.05.005
25. Kogelschatz U, Eliasson B, Egli W (1997) Dielectric-Barrier Discharges. Principle and Applications. J Phys IV France 07(C4):C4-47-C4-66. https://doi.org/10.1051/jp4:1997405
26. Becker KH, Kogelschatz U, Schoenbach KH, Barker RJ (eds) (2004) Non-Equilibrium Air Plasmas at Atmospheric Pressure, 0 edn. CRC Press
27. Tang Q, Jiang W, Cheng Y, Lin S, Lim TM, Xiong J (2011) Generation of Reactive Species by Gas-Phase Dielectric Barrier Discharges. Ind Eng Chem Res 50(17):9839–9846. https://doi.org/10.1021/ie200039w
28. Bruggeman P, Schram DC (2010) On OH production in water containing atmospheric pressure plasmas. Plasma Sources Sci Technol 19(4):045025. https://doi.org/10.1088/0963-0252/19/4/045025
29. Brandenburg R (2017) Dielectric barrier discharges: progress on plasma sources and on the understanding of regimes and single filaments. Plasma Sources Sci Technol 26(5):053001. https://doi.org/10.1088/1361-6595/aa6426
30. Mastanaiah N, Banerjee P, Johnson JA, Roy S (2013) Examining the Role of Ozone in Surface Plasma Sterilization Using Dielectric Barrier Discharge (DBD) Plasma: Examining the Role of Ozone in Surface Plasma Sterilization. Plasma Process Polym 10(12):1120–1133. https://doi.org/10.1002/ppap.201300108
31. Beutel BG, Danna NR, Gangolli R, Granato R, Manne L, Tovar N, Coelho PG (2014) Evaluation of bone response to synthetic bone grafting material treated with argon-based atmospheric pressure plasma. Materials Science and Engineering: C 45:484–490. https://doi.org/10.1016/j.msec.2014.09.039
32. Canal C, Modic M, Cvelbar U, Ginebra M-P (2016) Regulating the antibiotic drug release from β-tricalcium phosphate ceramics by atmospheric plasma surface engineering. Biomater Sci 4(10):1454–1461. https://doi.org/10.1039/C6BM00411C
33. Canal C, Gallinetti S, Ginebra M-P (2014) Low-Pressure Plasma Treatment of Polylactide Fibers for Enhanced Mechanical Performance of Fiber-Reinforced Calcium Phosphate Cements: Plasma Enhanced Mechanical Properties of PLA Fibre-Calcium Phosphate Cements. Plasma Process Polym 11(7):694–703. https://doi.org/10.1002/ppap.201400018
34. Trimukhe AM, Pandiyaraj KN, Tripathi A, Melo JS, Deshmukh RR (2017) Plasma Surface Modification of Biomaterials for Biomedical Applications. In: Tripathi A, Melo JS (eds) Advances in Biomaterials for Biomedical Applications. Springer Singapore, Singapore, pp 95–166
35. Cvelbar U, Canal C, Hori M (2017) Plasma-inspired biomaterials. J Phys D: Appl Phys 50(4):040201. https://doi.org/10.1088/1361-6463/50/4/040201

36. Miletic M, Mojsilovic S, Okic-Djordjevic I, Kukolj T, Jaukovic A, Santibacez JF, Jovcic G, Bugarski D (2014) Mesenchymal stem cells isolated from human periodontal ligament. Arch biol sci (Beogr) 66(1):261–271. https://doi.org/10.2298/ABS1401261M
37. Schlund M, Depeyre A, Kotagudda Ranganath S, Marchandise P, Ferri J, Chai F (2021) Rabbit calvarial and mandibular critical-sized bone defects as an experimental model for the evaluation of craniofacial bone tissue regeneration. Journal of Stomatology, Oral and Maxillofacial Surgery :S2468785521002688. https://doi.org/10.1016/j.jormas.2021.12.001
38. Manzini BM, Machado LMR, Noritomi PY, DA Silva JVL (2021) Advances in Bone tissue engineering: A fundamental review. J Biosci 46:17
39. Li Y, Jiang T, Zheng L, Zhao J (2017) Osteogenic differentiation of mesenchymal stem cells (MSCs) induced by three calcium phosphate ceramic (CaP) powders: A comparative study. Materials Science and Engineering: C 80:296–300. https://doi.org/10.1016/j.msec.2017.05.145
40. Saeed H, Ahsan M, Saleem Z, Iqtedar M, Islam M, Danish Z, Khan AM (2016) Mesenchymal stem cells (MSCs) as skeletal therapeutics–an update. J Biomed Sci 23(1):41. https://doi.org/10.1186/s12929-016-0254-3
41. Mushahary D, Spittler A, Kasper C, Weber V, Charwat V (2018) Isolation, cultivation, and characterization of human mesenchymal stem cells: hMSC. Cytometry 93(1):19–31. https://doi.org/10.1002/cyto.a.23242
42. Jin Y-Z, Lee JH (2018) Mesenchymal Stem Cell Therapy for Bone Regeneration. Clin Orthop Surg 10(3):271. https://doi.org/10.4055/cios.2018.10.3.271
43. Ruan S, Deng J, Yan L, Huang W (2018) Composite scaffolds loaded with bone mesenchymal stem cells promote the repair of radial bone defects in rabbit model. Biomedicine & Pharmacotherapy 97:600–606. https://doi.org/10.1016/j.biopha.2017.10.110
44. Šponer P, Kučera T, Brtková J, Urban K, Kočí Z, Měřička P, Bezrouk A, Konrádová Š, Filipová A, Filip S (2018) Comparative Study on the Application of Mesenchymal Stromal Cells Combined with Tricalcium Phosphate Scaffold into Femoral Bone Defects. Cell Transplant 27(10):1459–1468. https://doi.org/10.1177/0963689718794918
45. Blanco JF, Villarón EM, Pescador D, da Casa C, Gómez V, Redondo AM, López-Villar O, López-Parra M, Muntión S, Sánchez-Guijo F (2019) Autologous mesenchymal stromal cells embedded in tricalcium phosphate for posterolateral spinal fusion: results of a prospective phase I/II clinical trial with long-term follow-up. Stem Cell Res Ther 10(1):63. https://doi.org/10.1186/s13287-019-1166-4
46. Zhao Q, Li G, Wang T, Jin Y, Lu W, Ji J (2021) Human Periodontal Ligament Stem Cells Transplanted with Nanohydroxyapatite/Chitosan/Gelatin 3D Porous Scaffolds Promote Jaw Bone Regeneration in Swine. Stem Cells and Development 30(10):548–559. https://doi.org/10.1089/scd.2020.0204
47. Park J-Y, Jeon SH, Choung P-H (2011) Efficacy of Periodontal Stem Cell Transplantation in the Treatment of Advanced Periodontitis. Cell Transplant 20(2):271–286. https://doi.org/10.3727/096368910X519292

48. Kämmerer PW, Scholz M, Baudisch M, Liese J, Wegner K, Frerich B, Lang H (2017) Guided Bone Regeneration Using Collagen Scaffolds, Growth Factors, and Periodontal Ligament Stem Cells for Treatment of Peri-Implant Bone Defects In Vivo. Stem Cells International 2017:1–9. https://doi.org/10.1155/2017/3548435
49. Zhang Y, Xing Y, Jia L, Ji Y, Zhao B, Wen Y, Xu X (2018) An In Vitro Comparative Study of Multisource Derived Human Mesenchymal Stem Cells for Bone Tissue Engineering. Stem Cells and Development 27(23):1634–1645. https://doi.org/10.1089/scd.2018.0119
50. Kang H-J, Makkar P, Padalhin AR, Lee G-H, Im S-B, Lee B-T (2020) Comparative study on biodegradation and biocompatibility of multichannel calcium phosphate based bone substitutes. Materials Science and Engineering: C 110:110694. https://doi.org/10.1016/j.msec.2020.110694
51. Bohner M, Santoni BLG, Döbelin N (2020) β-tricalcium phosphate for bone substitution: Synthesis and properties. Acta Biomaterialia 113:23–41. https://doi.org/10.1016/j.actbio.2020.06.022
52. Dimitriou R, Tsiridis E, Giannoudis PV (2005) Current concepts of molecular aspects of bone healing. Injury 36(12):1392–1404. https://doi.org/10.1016/j.injury.2005.07.019
53. Kang Q, Song W-X, Luo Q, Tang N, Luo J, Luo X, Chen J, Bi Y, He B-C, Park JK, Jiang W, Tang Y, Huang J, Su Y, Zhu G-H, He Y, Yin H, Hu Z, Wang Y, Chen L, Zuo G-W, Pan X, Shen J, Vokes T, Reid RR, Haydon RC, Luu HH, He T-C (2009) A Comprehensive Analysis of the Dual Roles of BMPs in Regulating Adipogenic and Osteogenic Differentiation of Mesenchymal Progenitor Cells. Stem Cells and Development 18(4):545–558. https://doi.org/10.1089/scd.2008.0130
54. Dorman LJ, Tucci M, Benghuzzi H (2012) In vitro effects of bmp-2, bmp-7, and bmp-13 on proliferation and differentation of mouse mesenchymal stem cells. Biomed Sci Instrum 48:81–87
55. Garg P, Mazur MM, Buck AC, Wandtke ME, Liu J, Ebraheim NA (2017) Prospective Review of Mesenchymal Stem Cells Differentiation into Osteoblasts: Mesenchymal Stem Cells Differentiation. Orthop Surg 9(1):13–19. https://doi.org/10.1111/os.12304
56. Salazar VS, Gamer LW, Rosen V (2016) BMP signalling in skeletal development, disease and repair. Nat Rev Endocrinol 12(4):203–221. https://doi.org/10.1038/nrendo.2016.12
57. Millan C, Vivanco JF, Benjumeda-Wijnhoven IM, Bjelica S, Santibanez JF (2018) Mesenchymal Stem Cells and Calcium Phosphate Bioceramics: Implications in Periodontal Bone Regeneration. In: Turksen K (ed) Cell Biology and Translational Medicine, Volume 3. Springer International Publishing, Cham, pp 91–112
58. Linsley C, Wu B, Tawil B (2013) The Effect of Fibrinogen, Collagen Type I, and Fibronectin on Mesenchymal Stem Cell Growth and Differentiation into Osteoblasts. Tissue Engineering Part A 19(11–12):1416–1423. https://doi.org/10.1089/ten.tea.2012.0523
59. Somaiah C, Kumar A, Mawrie D, Sharma A, Patil SD, Bhattacharyya J, Swaminathan R, Jaganathan BG (2015) Collagen Promotes Higher Adhesion, Survival and Proliferation of Mesenchymal Stem Cells. PLoS ONE 10(12):e0145068. https://doi.org/10.1371/journal.pone.0145068
60. Ribeiro N, Sousa SR, Brekken RA, Monteiro FJ (2014) Role of SPARC in Bone Remodeling and Cancer-Related Bone Metastasis: SPARC in Bone Remodeling and Bone Metastasis. J Cell Biochem

115(1):17–26. https://doi.org/10.1002/jcb.24649

61. Samavedi S, Whittington AR, Goldstein AS (2013) Calcium phosphate ceramics in bone tissue engineering: A review of properties and their influence on cell behavior. Acta Biomaterialia 9(9):8037–8045. https://doi.org/10.1016/j.actbio.2013.06.014
62. Salamanca E, Pan Y-H, Tsai A, Lin P-Y, Lin C-K, Huang H-M, Teng N-C, Wang P, Chang W-J (2017) Enhancement of Osteoblastic-Like Cell Activity by Glow Discharge Plasma Surface Modified Hydroxyapatite/β-Tricalcium Phosphate Bone Substitute. Materials 10(12):1347. https://doi.org/10.3390/ma10121347
63. Canullo L, Genova T, Naenni N, Nakajima Y, Masuda K, Mussano F (2018) Plasma of argon enhances the adhesion of murine osteoblasts on different graft materials. Annals of Anatomy - Anatomischer Anzeiger 218:265–270. https://doi.org/10.1016/j.aanat.2018.03.005
64. Fu X, Jenkins MJ, Sun G, Bertoti I, Dong H (2012) Characterization of active screen plasma modified polyurethane surfaces. Surface and Coatings Technology 206(23):4799–4807. https://doi.org/10.1016/j.surfcoat.2012.04.051
65. Jeong J, Kim JH, Shim JH, Hwang NS, Heo CY (2019) Bioactive calcium phosphate materials and applications in bone regeneration. Biomater Res 23(1):4. https://doi.org/10.1186/s40824-018-0149-3
66. Lee D-S, Moriguchi Y, Okada K, Myoui A, Yoshikawa H, Hamaguchi S (2011) Improvement of Hydrophilicity of Interconnected Porous Hydroxyapatite by Dielectric Barrier Discharge Plasma Treatment. IEEE Trans Plasma Sci 39(11):2166–2167. https://doi.org/10.1109/TPS.2011.2157840
67. Zhao G, Schwartz Z, Wieland M, Rupp F, Geis-Gerstorfer J, Cochran DL, Boyan BD (2005) High surface energy enhances cell response to titanium substrate microstructure. J Biomed Mater Res 74A(1):49–58. https://doi.org/10.1002/jbm.a.30320
68. Hamlet S, Alfarsi M, George R, Ivanovski S (2012) The effect of hydrophilic titanium surface modification on macrophage inflammatory cytokine gene expression. Clin Oral Impl Res 23(5):584–590. https://doi.org/10.1111/j.1600-0501.2011.02325.x
69. Hotchkiss KM, Reddy GB, Hyzy SL, Schwartz Z, Boyan BD, Olivares-Navarrete R (2016) Titanium surface characteristics, including topography and wettability, alter macrophage activation. Acta Biomaterialia 31:425–434. https://doi.org/10.1016/j.actbio.2015.12.003
70. Hotchkiss KM, Sowers KT, Olivares-Navarrete R (2019) Novel in vitro comparative model of osteogenic and inflammatory cell response to dental implants. Dental Materials 35(1):176–184. https://doi.org/10.1016/j.dental.2018.11.011
71. Leuning DG, Beijer NRM, du Fossé NA, Vermeulen S, Lievers E, van Kooten C, Rabelink TJ, Boer J de (2018) The cytokine secretion profile of mesenchymal stromal cells is determined by surface structure of the microenvironment. Sci Rep 8(1):7716. https://doi.org/10.1038/s41598-018-25700-5
72. Abagnale G, Steger M, Nguyen VH, Hersch N, Sechi A, Joussen S, Denecke B, Merkel R, Hoffmann B, Dreser A, Schnakenberg U, Gillner A, Wagner W (2015) Surface topography enhances differentiation of mesenchymal stem cells towards osteogenic and adipogenic lineages. Biomaterials 61:316–326. https://doi.org/10.1016/j.biomaterials.2015.05.030

73. Zhang Y, Böse T, Unger RE, Jansen JA, Kirkpatrick CJ, van den Beucken JJJP (2017) Macrophage type modulates osteogenic differentiation of adipose tissue MSCs. Cell Tissue Res 369(2):273–286. https://doi.org/10.1007/s00441-017-2598-8
74. Gamblin A-L, Brennan MA, Renaud A, Yagita H, Lézot F, Heymann D, Trichet V, Layrolle P (2014) Bone tissue formation with human mesenchymal stem cells and biphasic calcium phosphate ceramics: The local implication of osteoclasts and macrophages. Biomaterials 35(36):9660–9667. https://doi.org/10.1016/j.biomaterials.2014.08.018
75. Wang M, Yuan Q, Xie L (2018) Mesenchymal Stem Cell-Based Immunomodulation: Properties and Clinical Application. Stem Cells International 2018:1–12. https://doi.org/10.1155/2018/3057624
76. Freytes DO, Kang JW, Marcos-Campos I, Vunjak-Novakovic G (2013) Macrophages modulate the viability and growth of human mesenchymal stem cells. J Cell Biochem 114(1):220–229. https://doi.org/10.1002/jcb.24357
77. Viti F, Landini M, Mezzelani A, Petecchia L, Milanesi L, Scaglione S (2016) Osteogenic Differentiation of MSC through Calcium Signaling Activation: Transcriptomics and Functional Analysis. PLoS ONE 11(2):e0148173. https://doi.org/10.1371/journal.pone.0148173
78. Tour G, Wendel M, Tcacencu I (2014) Bone marrow stromal cells enhance the osteogenic properties of hydroxyapatite scaffolds by modulating the foreign body reaction: BMSCs modulate foreign body reaction. J Tissue Eng Regen Med 8(11):841–849. https://doi.org/10.1002/term.1574

Figures

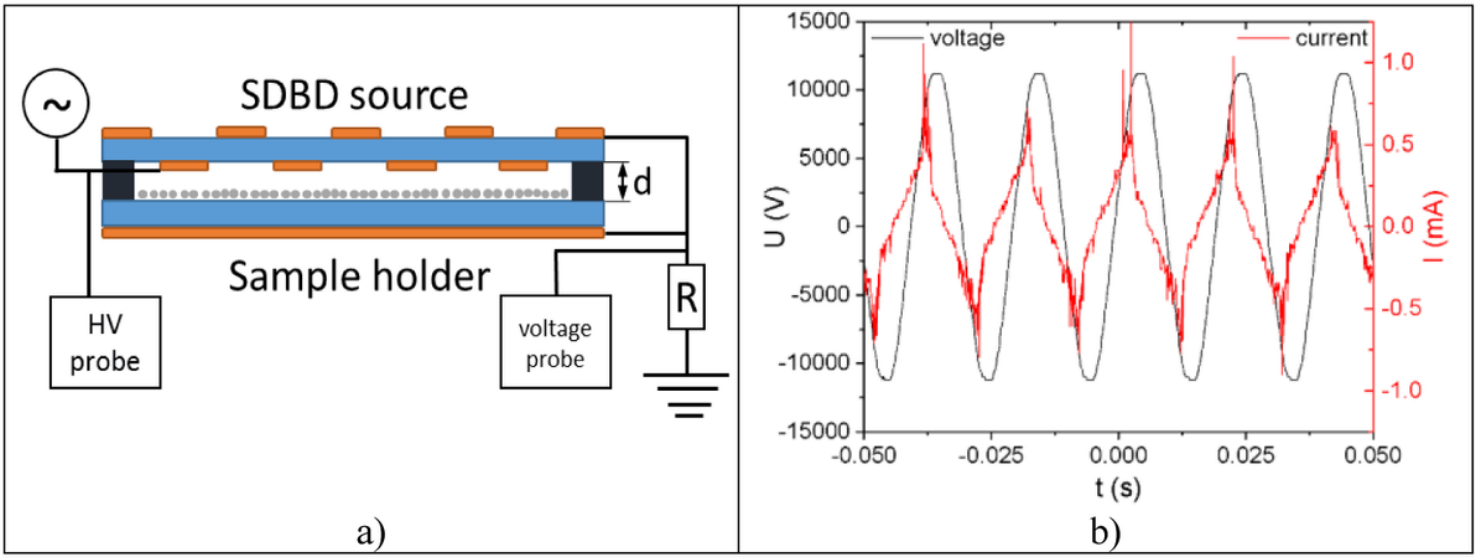

Figure 1

Experimental setup. a) Schematics of surface dielectric barrier discharge (SDBD) system b) Voltage and current waveforms.

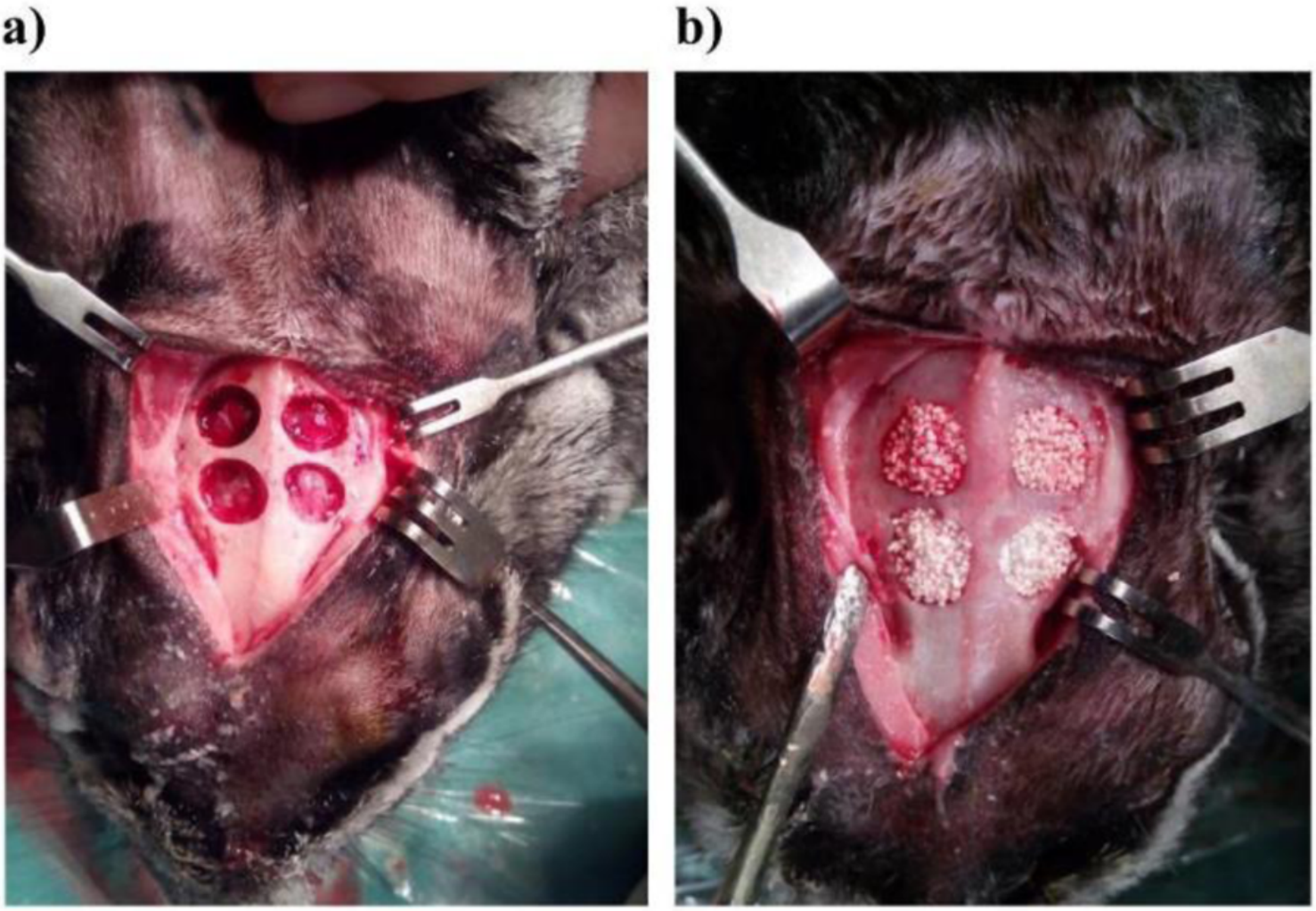

Figure 2

Calvarial critical-sized defects of 8 mm of diameter in a rabbit model, a) before and b) after implantation.

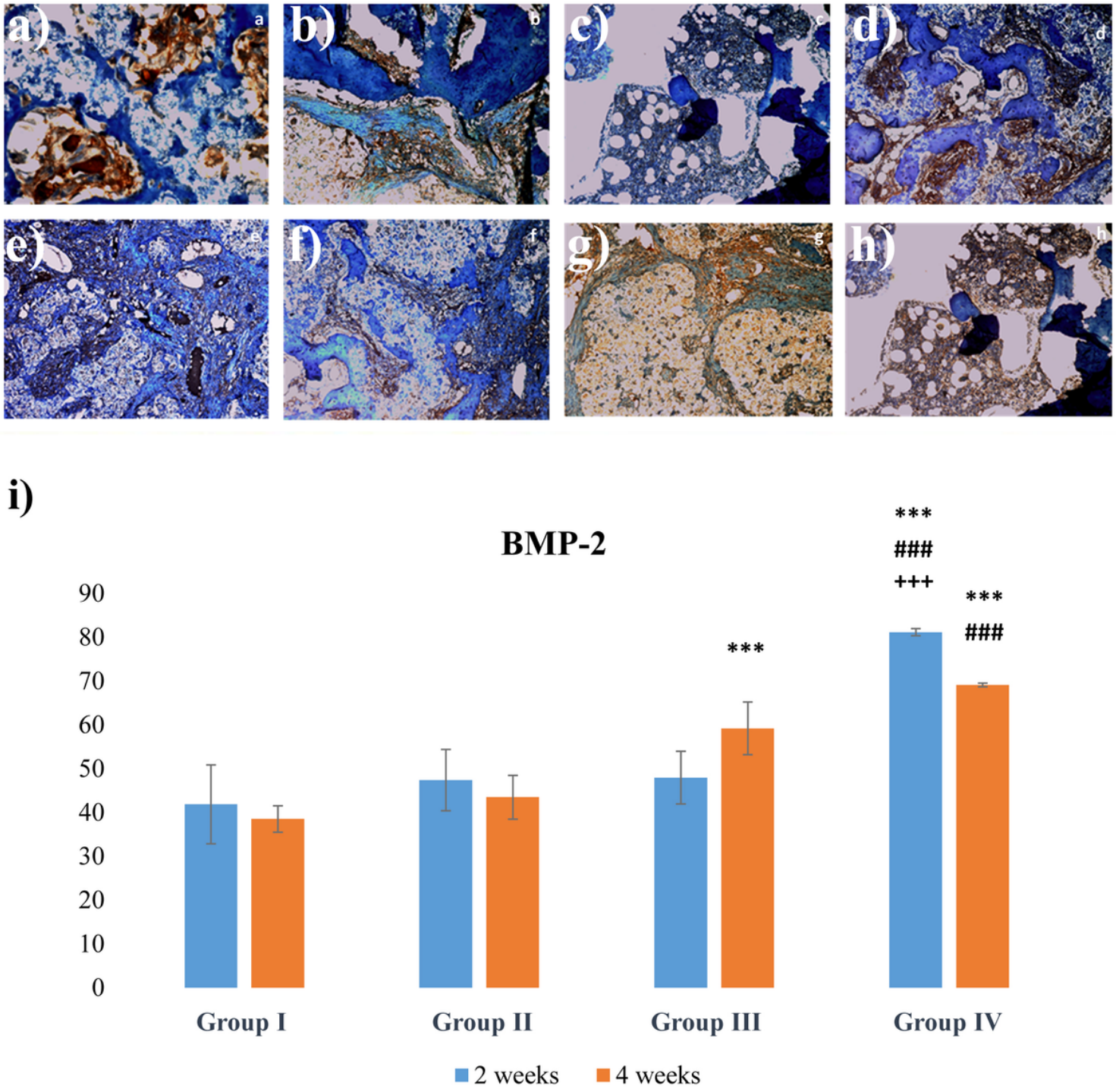

Figure 3

Immunohistochemical analysis of BMP-2 positive cells in the defects after 2 (a, b, c, d) and 4 (e, f, g, h) weeks postoperatively: a, e - group I - β-TCP; b, f - group II - plasma-treated β-TCP; c, g - group III - β-TCP and PDLSCs; d, h - group IV - plasma-treated β-TCP and PDLSCs. (i) Median values of immunostaining calculated by determining the BMP-2-positive areas (brown-colored cells) are presented on the graph. ***, $p < 0,001$ - compared with group I; ###, $p < 0,001$ - compared with group II; +++, $p < 0,001$ - compared with group III.

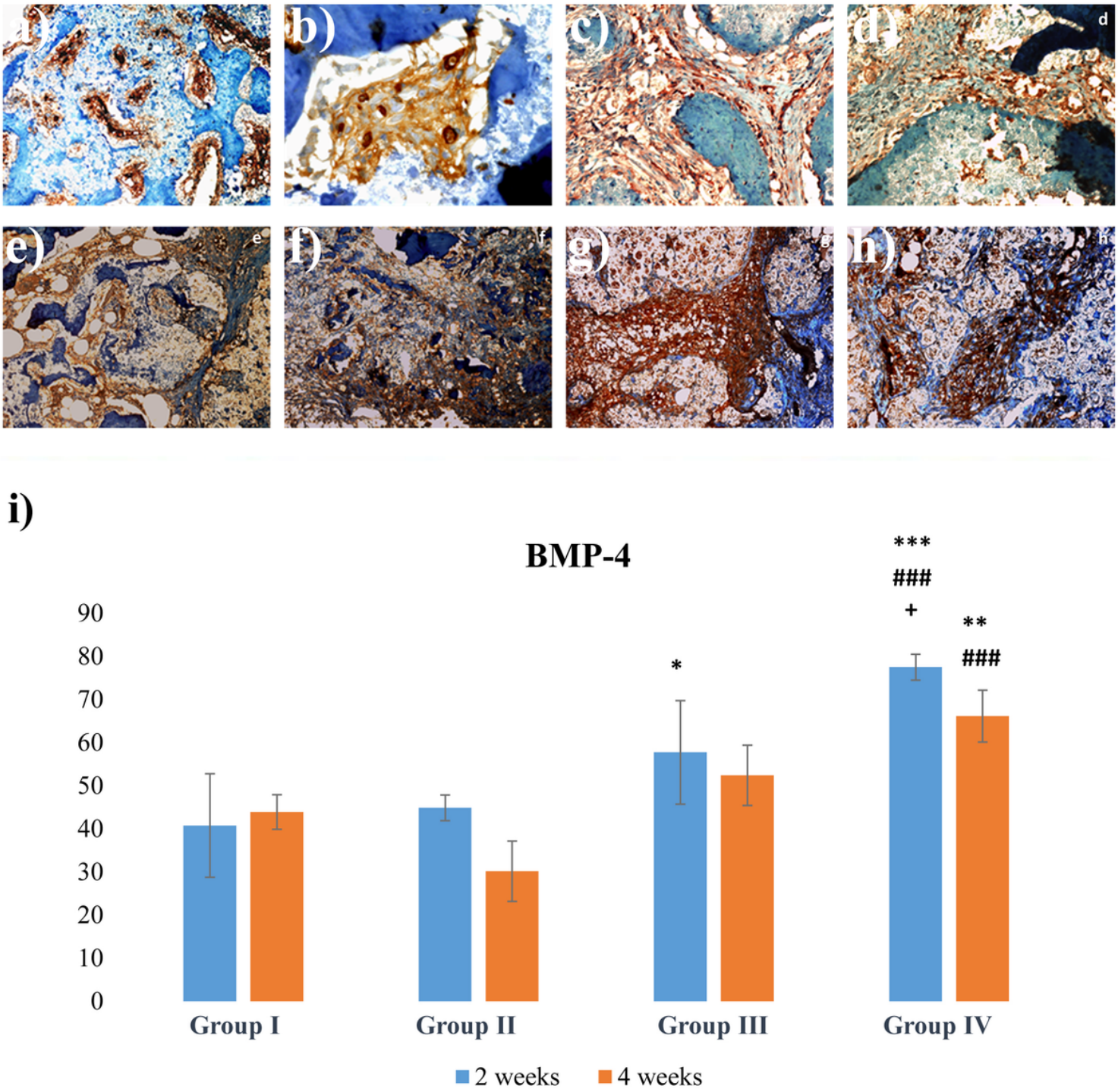

Figure 4

Immunohistochemical analysis of BMP-4 positive cells in the defects after 2 (a, b, c, d) and 4 (e, f, g, h) weeks postoperatively: a, e - group I - β-TCP; b, f - group II - plasma-treated β-TCP; c, g - group III - β-TCP and PDLSCs; d, h - group IV - plasma-treated β-TCP and PDLSCs. (i) Median values of immunostaining calculated by determining the BMP-4-positive areas (brown-colored cells) are presented on the graph. *, $p < 0,05$; **, $p < 0,01$; ***, $p < 0,001$-compared with group I; ###, $p < 0,001$-compared with group II; +, $p < 0,05$-compared with group III.

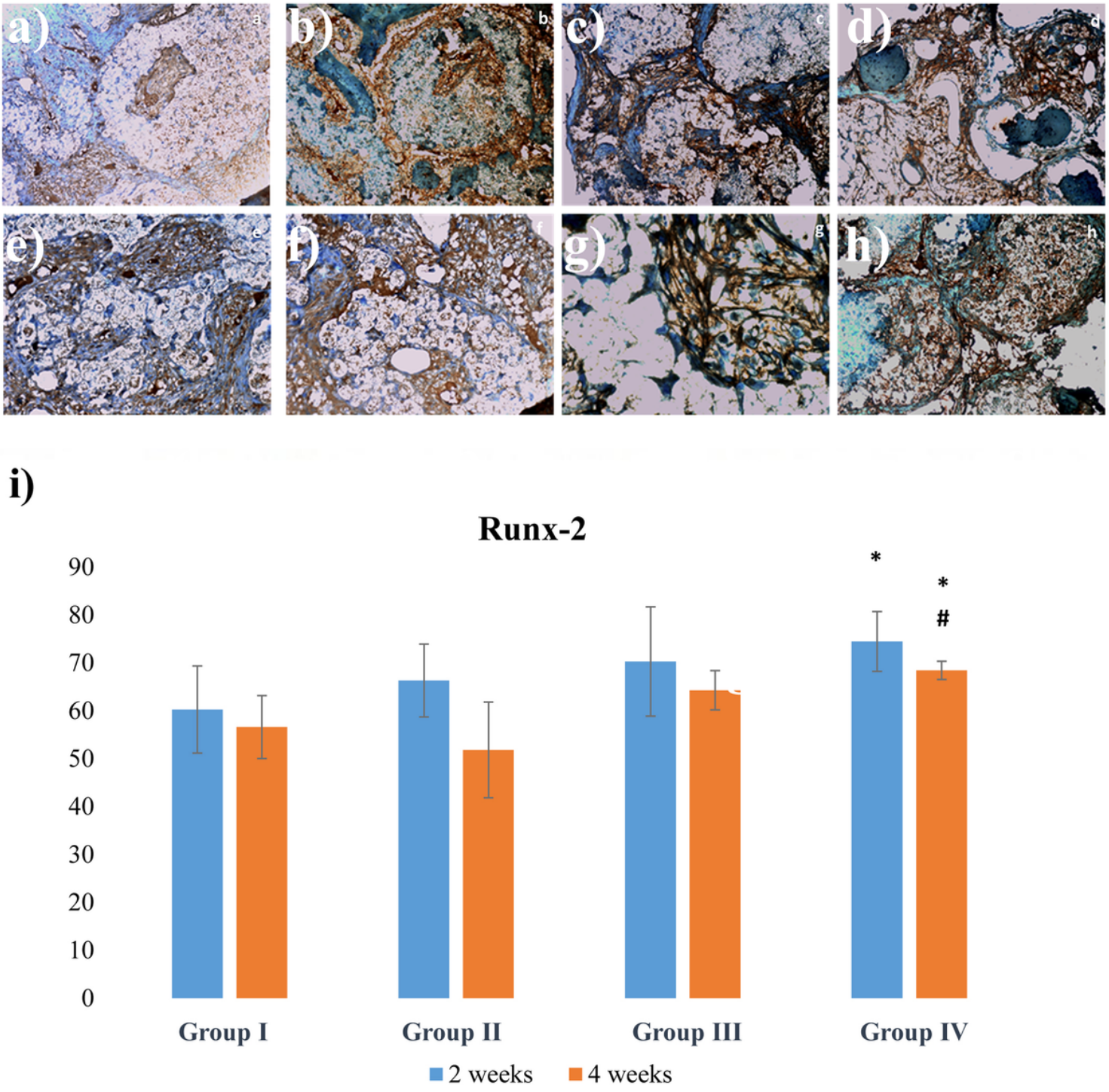

Figure 5

Immunohistochemical analysis of Runx-2 positive cells in the defects after 2 (a, b, c, d) and 4 (e, f, g, h) weeks postoperatively: a, e - group I - β-TCP; b, f - group II - plasma-treated β-TCP; c, g - group III - β-TCP and PDLSCs; d, h - group IV - plasma-treated β-TCP and PDLSCs. (i) Median values of immunostaining calculated by determining the Runx-2-positive areas (brown-colored cells) are presented on the graph. *, $p < 0,05$ - compared with group I; #, $p < 0,05$ - compared with group II.

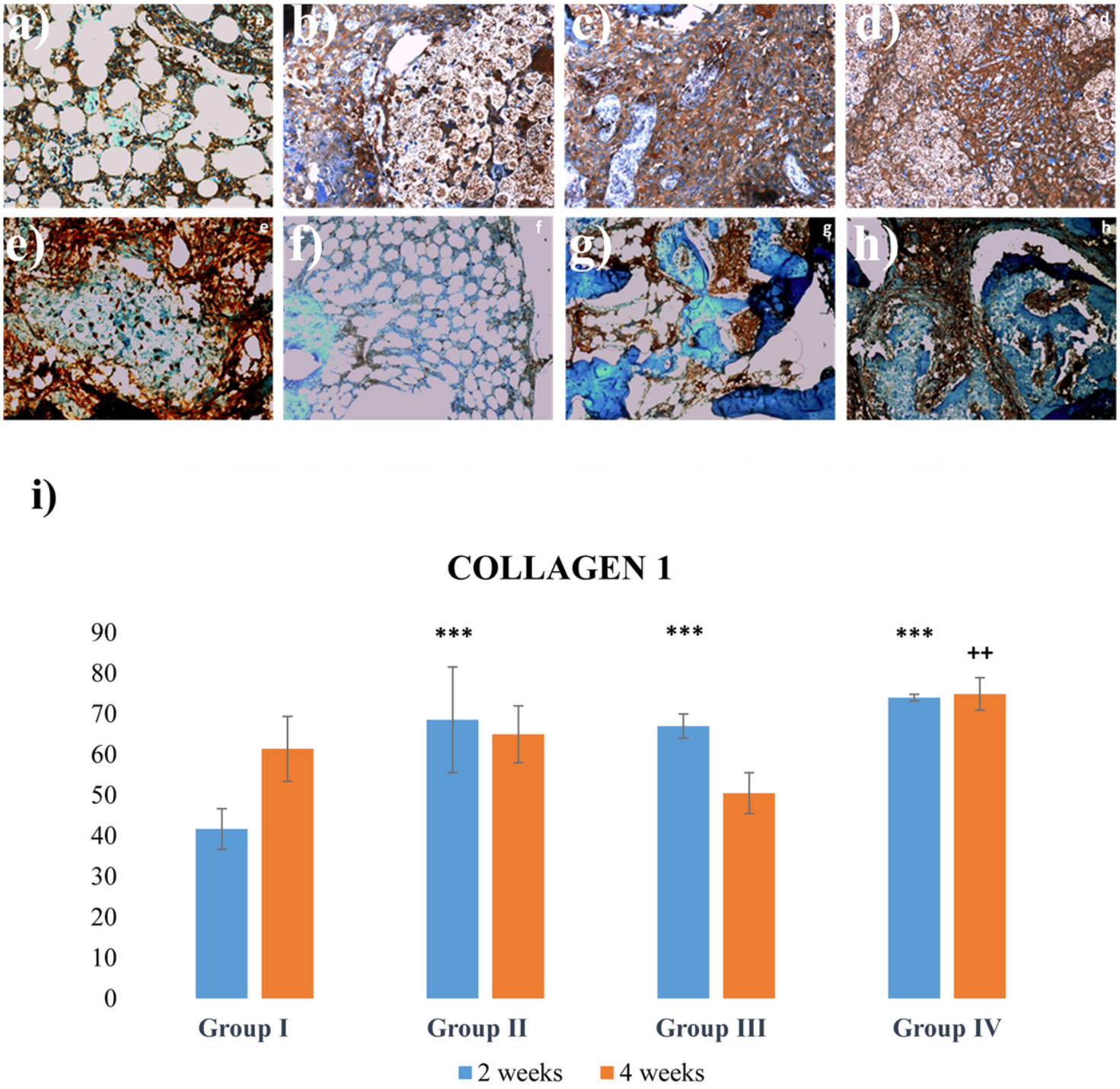

Figure 6

Immunohistochemical analysis of collagen-1-positive cells in the defects after 2 (a, b, c, d) and 4 (e, f, g, h) weeks postoperatively: a, e - group I - β-TCP; b, f - group II - plasma-treated β-TCP; c, g - group III - β-TCP and PDLSCs; d, h - group IV - plasma-treated β-TCP and PDLSCs. (i) Median values of immunostaining calculated by determining the collagen-1-positive areas (brown-colored cells) are presented on the graph. ***, $p < 0,001$- compared with group I; ++, $p < 0,01$- compared with group III.

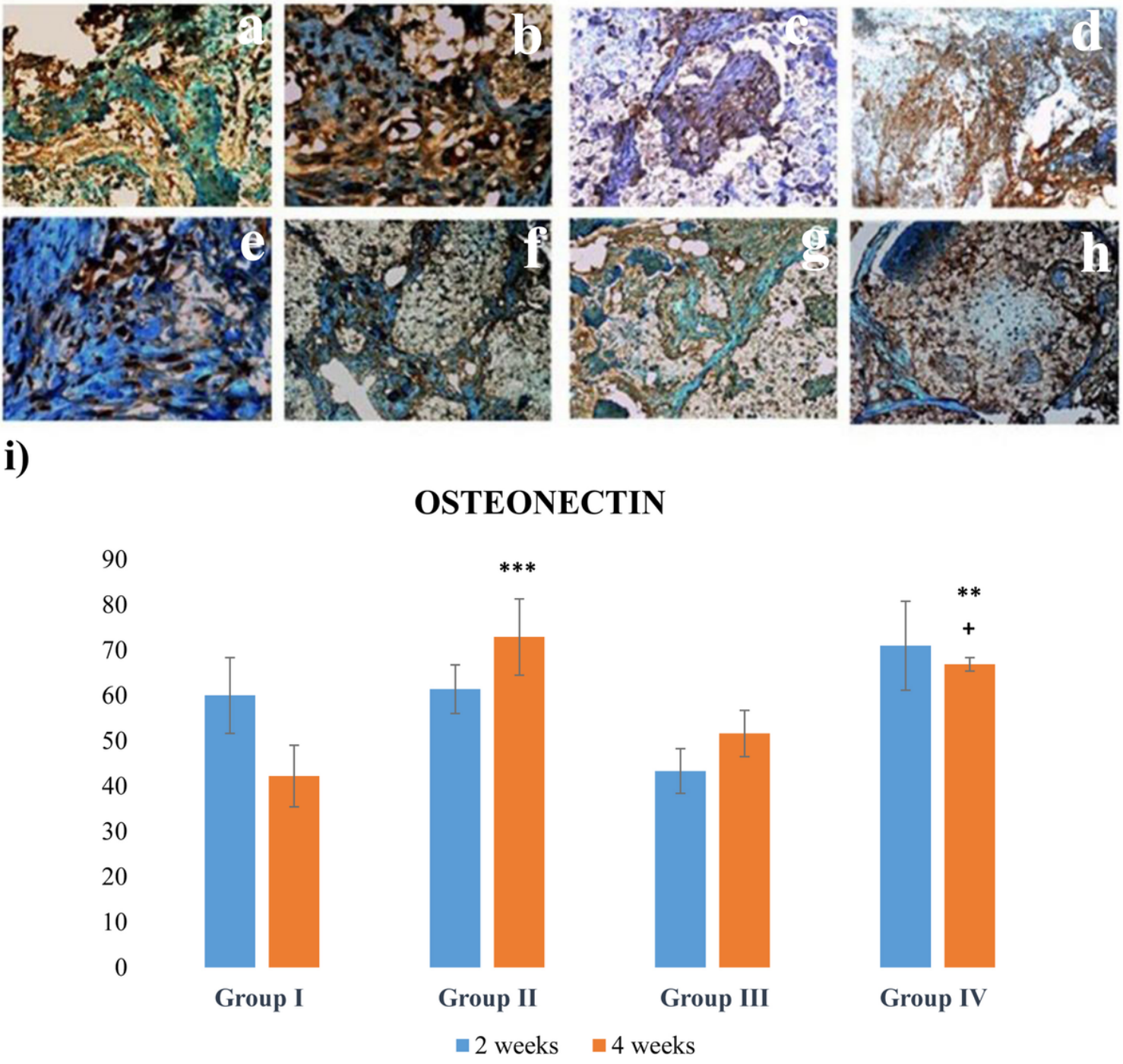

Figure 7

Immunohistochemical analysis of osteonectin positive cells in the defects after 2 (a, b, c, d) and 4 (e, f, g, h) weeks postoperatively: a, e - group I - β-TCP; b, f - group II - plasma-treated β-TCP; c, g - group III - β-TCP and PDLSCs; d, h - group IV - plasma-treated β-TCP and PDLSCs. (i) Median values of immunostaining calculated by determining the osteonectin-positive areas (brown-colored cells) are presented on the graph. **, $p < 0,01$; ***, $p < 0,001$ - compared with group I; +, $p < 0,05$ - compared with group III.